DEGAS: Detailed Expressions on Full-Body Gaussian Avatars

Zhijing Shao[1,2] Duotun Wang[1] Qing-Yao Tian[2] Yao-Dong Yang[1] Hengyu Meng[1]
Zeyu Cai[1] Bo Dong[4] Yu Zhang[2] Kang Zhang[1,3] Zeyu Wang[1,3]
[1]The Hong Kong University of Science and Technology (Guangzhou)
[2]Prometheus Vision Technology Co., Ltd.
[3]The Hong Kong University of Science and Technology
[4]Swinburne University of Technology

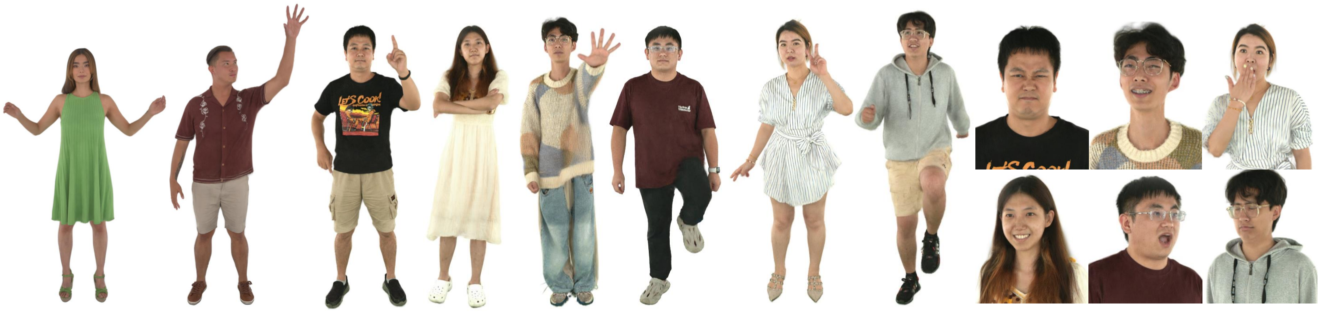
(a) ActorsHQ dataset rendered by DEGAS (b) Our DREAMS-Avatar dataset rendered by DEGAS (c) Rich facial expressions rendered by DEGAS

Figure 1. **Photorealistic rendering of full-body avatars using our method on (a) ActorsHQ dataset and (b) our proposed DREAMS-Avatar dataset, (c) with rich facial expressions.**

Abstract

Although neural rendering has made significant advances in creating lifelike, animatable full-body and head avatars, incorporating detailed expressions into full-body avatars remains largely unexplored. We present DEGAS, the first 3D Gaussian Splatting (3DGS)-based modeling method for full-body avatars with rich facial expressions. Trained on multiview videos of a given subject, our method learns a conditional variational autoencoder that takes both the body motion and facial expression as driving signals to generate Gaussian maps in the UV layout. To drive the facial expressions, instead of the commonly used 3D Morphable Models (3DMMs) in 3D head avatars, we propose to adopt the expression latent space trained solely on 2D portrait images, bridging the gap between 2D talking faces and 3D avatars. Leveraging the rendering capability of 3DGS and the rich expressiveness of the expression latent space, the learned avatars can be reenacted to reproduce photorealistic rendering images with subtle and accurate facial expressions. Experiments on an existing dataset and our newly proposed dataset of full-body talking avatars demonstrate the efficacy of our method. We also propose an audio-driven extension of our method with the help of 2D talking faces, opening new possibilities for interactive AI agents. Project page: https://initialneil.github.io/DEGAS.

1. Introduction

Photorealistic and animatable human modeling has been an active research topic in computer vision and graphics for decades. Interactive avatars that are capable of performing natural body motions and subtle facial expressions can benefit numerous downstream applications, e.g., telepresentation [30, 34], virtual companion [3], and extended reality (XR) storytelling [8, 22].

With the rise of neural rendering such as Neural Radiance Fields (NeRF) [42] and 3DGS [31], we observe a boost in terms of quality and rendering efficiency for both *full-body avatars* [25, 29, 38] and *head avatars* [52, 55, 56, 80]. Yet there is a lack of dataset and method for integrating the *two*, i.e., expressive full-body avatars equipped with both body pose control and rich facial expressions. We aim to fill in the gap by proposing **DEGAS** (**D**etailed **E**xpressions on full-body **G**aussian **A**vatar**s**), the first 3DGS-based method for modeling full-body talking avatars together with a new dataset for evaluation.

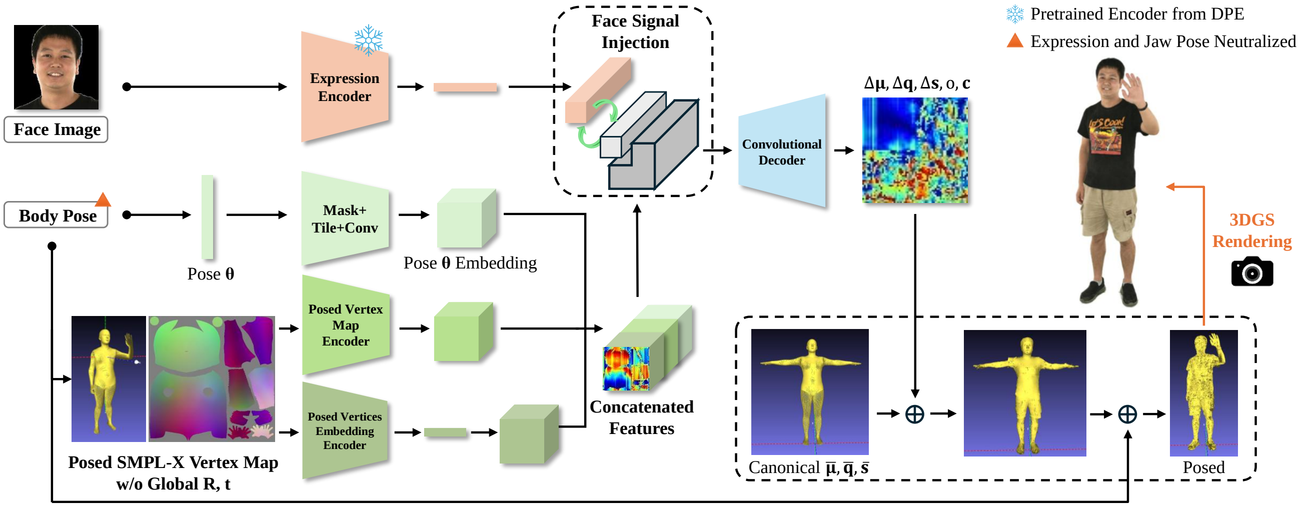
Face Image
Expression Encoder
Face Signal Injection
Pretrained Encoder from DPE
Expression and Jaw Pose Neutralized
$\Delta\mathbf{\mu}, \Delta\mathbf{q}, \Delta\mathbf{s}, o, \mathbf{c}$
Convolutional Decoder
Body Pose
Pose $\boldsymbol{\theta}$
Mask+ Tile+Conv
Pose $\boldsymbol{\theta}$ Embedding
3DGS Rendering
Posed Vertex Map Encoder
Posed Vertices Embedding Encoder
Concatenated Features
Posed SMPL-X Vertex Map w/o Global R, t
Canonical $\bar{\mathbf{\mu}}, \bar{\mathbf{q}}, \bar{\mathbf{s}}$
Posed

Figure 2. **The pipeline of our method.** DEGAS takes face signal from the pretrained expression encoder of DPE [44], which is injected to the body signal from SMPL-X [46]. The pose-dependent Gaussian maps generated by the convolutional decoder are applied to the pose-independent maps for 3DGS [31] rendering.

A naive way to enable facial expressions on full-body avatars would be using 3DMMs for facial control, for example, controlling the *expression* parameters of SMPL-X [46], or using the parameters of FLAME [36] or BFM [47] as driving signals. We find two drawbacks of such naive methods. 1) The expressiveness of 3DMMs is limited [44, 59, 65]. Being coarse meshes, 3DMMs are essentially not able to capture subtle facial changes. 2) Driving signal generation for a 3DMM is non-trivial. Both video-driven [17, 41, 78] and audio-driven [1, 16, 50, 58, 65] methods suffer from efficiency, accuracy, and expressiveness issues. Recent works [43, 52] have achieved photorealistic facial modeling in a very dense multi-view camera set-up. However, accurate 3DMM registration is non-trivial from a monocular camera [17, 41].

One important trend we observe in recent works on 2D talking faces is the learning of disentangled latent spaces for identity, pose, and expression [15, 44, 62, 68]. Such a framework enables standalone extraction of identity-agnostic pose and expression parameters from input images. We propose to adopt the pretrained encoder for expression from DPE [44] to generate driving signals for the facial control of our avatar modeling. To the best of our knowledge, we are the first method to bridge the gap between 2D talking faces and 3D avatars. We take inspiration from the Score Distillation Sampling proposed in DreamFusion [51] where a pretrained 2D generative model lays the foundation for 3D generative tasks.

One of the benefits of involving a pretrained encoder is that we can extend audio-driven 2D talking faces to our 3D avatars. Given one portrait image and an audio clip, we first use SadTalker [74] to generate the corresponding talking head video, and then apply the pretrained expression encoder to extract driving signals for our avatars.

Though both trained with registered meshes, head avatars and full-body avatars usually face very different registration qualities. With well aligned mesh surfaces, the binding of the 3D Gaussians and the underlying mesh is usually simple for head avatars. Both SplattingAvatar [56] and GaussianAvatars [52] propose to bind 3D Gaussians to FLAME mesh triangles without any pose-dependent compensations. Full-body avatars, on the other hand, usually face the challenge of a much less accurate underlying mesh because of clothing. D3GA [79] proposes to alleviate this problem by modeling clothes with separate tetrahedron layers. We follow the practice of AnimatableGaussians [38] and CodecAvatars [2] to leverage the ability of 2D CNNs for the pose-dependent generation of 3DGS parameters.

In summary, our main contributions are as follows:

- We propose the first 3DGS-based method for full-body talking avatars and a multi-view captured dataset of full-body avatars with rich facial expressions.
- We propose to drive 3D avatars with 2D talking faces, bridging the gap between these two research topics and opening new possibilities for the reenactment of photo-realistic avatars.

2. Related Work

2.1. 3D Avatar Representations

3D avatar modeling methods have three major design choices to make: appearance representation, canonical modeling, and posing method. The change of appearance representation from mesh texture [2, 20, 40] to points [75], NeRF [29, 80], and 3DGS [25, 38, 52, 56], has been the driving force of quality improvements in this field.

In terms of canonical modeling, there are two major categories depending on whether the appearance is pixel-wisely defined on the UV space or not. UV atlas of SMPL [39], SMPL-X [46], and FLAME [36] provides a well aligned layout for pixel-wise appearance representation. CodecAvatars [2, 40, 43], HDHumans [21], DDC [20], and UVVolumes [7] predict pixel-wise appearance features on the UV space. RGCA [55], ASH [45], and GaussianAvatar [25] construct pixel-wise 3D Gaussian parameters. AnimatableGaussians [38] further uses front and back planes to utilize the geometry details from the mesh.

When the UV layout is not used, the canonical model is usually defined tightly aligned to the underlying mesh. NeuralBody [48, 49] encodes learnable latent codes to SMPL mesh vertices. EditableHumans [24] assigns a learnable codebook to the vertices of SMPL-X. SLRF [76] learns structured local radiance fields attached to SMPL. AvatarRex [77] models the appearance with feature planes aligned to the canonical mesh. TAVA [35], TotalSelfScan [13], PoseVocab [37], InstantAvatar [29], and INSTA [80] propose to build NeRF aligned with the canonical mesh. PointAvatar [75] constructs canonical points coupled with FLAME canonical space. ARAH [60] and X-Avatar [57] define pose-conditioned colors on the surface of the canonical SDF. SplattingAvatar [56] and GaussianAvatars [52] learn 3D Gaussians embedded on the underlying mesh triangles. 3DGS-Avatar [53] and GauHuman [26] initialize 3D Gaussians by sampling from SMPL. To take advantage of powerful 2D CNNs, our method falls in the former category with pixel-wise 3DGS parameters defined as UV maps.

With the appearance and canonical modeling chosen, the posing scheme helps warp sample points from the canonical space to the posed space or vice versa depending on the need for rendering. Posed-dependent compensation is usually introduced together with LBS to achieve higher quality [2, 25, 38, 40, 55], while direct posing from mesh triangles increases the inference FPS [52, 56, 80]. Appearance modeling methods of texture, points, and 3DGS favor a forward posing scheme, i.e., per-primitive conversion from the canonical space to the posed space. NeRF-based methods [13, 29, 35, 37], on the other hand, usually require the conversion of multiple samples on each ray from the posed space back to the canonical space [5, 6].

2.2. Talking Face Video Generation

With rapid advances in GANs and diffusion models, talking-face video generation has achieved remarkable quality improvements. For instance, view-dependent landmarks [61] and 3DMMs [70] have been leveraged to enhance the temporal consistency of synthesized facial animations. Recent investigations have focused on distilling disentangled information such as emotion [4, 66], expression [44], and appearance [72], enabling face reenactment and editing across identities. For producing different speaking styles, image translation approaches [18, 28] are utilized (e.g., HeadGAN [14] and SadTalker [74]). To express a realistic appearance with natural pose modifications, researchers have extended NeRF and 3DGS to talking face tasks, as seen in GaussianTalk [71] and Ad-NeRF [19].

2.3. Choice of Driving Signal

Different from a 4D playback system like FVV [10], or 4DGS [64], avatar modeling methods focus on the reenactment from accessible driving signals. For full-body avatars, apart from the commonly used skeleton poses as driving signals [25, 29, 53], AnimatableGaussians [38] also encodes the posed position maps. SurMo [27] further considers temporal dynamics to overcome the limitation of the deterministic nature of driving signals. Head avatars [52, 56, 75, 80], on the other hand, usually take into account the expression parameters of the underlying 3DMMs for better capturing the surface deformation of the face mesh. Audio2Photoreal [43] models mesh-based full-body avatars with facial control of accurate expression parameters registered from a dense camera set-up, which is non-trivial to acquire from a more casual set-up.

Recent works in talking face video generation have explored different driving signals for both audio-driven and video-driven tasks. Some [50, 54, 70] follow the practice of 3D face animation [11, 16, 58, 65] to use parameters from a pretrained 3DMM as the driving signal. However, the expressiveness of 3DMM is limited. CodeTalker [65] proposes to regress vertex offsets instead of FLAME parameters to improve the expressiveness of face animation. DPE [44], instead of using 3DMMs, designs a bidirectional cyclic training strategy to construct disentangled latent spaces for pose and expression. VASA-1 [68] and Hallo [67] inherit this idea and achieve outstanding quality with the diffusion model. In this paper, we aim to discuss that a well-trained latent space of expression solely from 2D images, is a better choice than 3DMM as the driving signal to reenact expressive 3D avatars.

3. Methodology

Given synchronized multiview videos and per-frame registered SMPL-X of a given subject, we train an expressive full-body avatar modeled by a conditional variational autoencoder (cVAE) to generate the 3D Gaussian maps in the layout of SMPL-X's UV space, where each pixel parameterizes one 3D Gaussian primitive. We briefly introduce 3DGS in Section 3.1, and elaborate on the choice of driving signals in Section 3.2, the design of cVAE in Section 3.3, the LBS-based posing scheme in Section 3.4, and finally the training process in Section 3.5.

3.1. Preliminaries: 3D Gaussian Splatting

3DGS [31] is an explicit primitive-based 3D representation that models a scene or an object by a set of semi-transparent ellipsoids as 3D Gaussians. Each 3D Gaussian has a parameter set of $G_i = (\boldsymbol{\mu}_i, \boldsymbol{q}_i, \boldsymbol{s}_i, o_i, \boldsymbol{\eta}_i)$. The probability density of each Gaussian in space is formulated by its mean (position) $\boldsymbol{\mu}_i$ and covariance matrix Σ_i as:

$$f(x|\boldsymbol{\mu}_i, \Sigma_i) = e^{-\frac{1}{2}(x-\boldsymbol{\mu}_i)^T \Sigma_i^{-1}(x-\boldsymbol{\mu}_i)} \tag{1}$$

$$\Sigma_i = R_i S_i S_i^T R_i^T \tag{2}$$

where the rotation matrix R_i and scaling matrix S_i that formulate the covariance matrix Σ_i are constructed from the rotation quaternion $\boldsymbol{q}_i$ and the scaling vector $\boldsymbol{s}_i$ respectively.

Given the world-to-camera view matrix W and the Jacobian J of the point projection matrix, the influence of the 3D Gaussians can be splatted onto 2D [81]:

$$\Sigma'_i = JW\Sigma_i W^T J^T \tag{3}$$

The final rendered color $\boldsymbol{C}$ of a pixel is given by the α-*blending* of the 3D Gaussians that splatted onto it from near to far:

$$\boldsymbol{C} = \sum_{i=1}^{N} \boldsymbol{c_i}\alpha_i \prod_{j=1}^{i-1}(1-\alpha_j) \tag{4}$$

with α_i evaluated from the splatted covariance Σ'_i, and the opacity in logit o_i with sigm() being the standard sigmoid function:

$$\alpha_i(x) = \text{sigm}(o_i)\exp(-\frac{1}{2}(x-\mu_i)(\Sigma'_i)^{-1}(x-\mu_i)) \tag{5}$$

and $\boldsymbol{c_i}$ is the view-dependent color represented by spherical harmonics $\boldsymbol{\eta}_i$. For simplicity in this paper, we disable the view-dependent components of $\boldsymbol{\eta}_i$ by predicting $\boldsymbol{c_i}$ directly.

3.2. Driving Signal

For full-body talking avatars, both facial expressions and body gestures convey important messages in the process of communication. We divide the driving signals into two parts: body signal and face signal.

Body signal. We use the body pose parameters from SMPL-X as the body signal, which enables body motion control down to the finger level. We keep the motion of the head to make the avatar more natural. The jaw pose, on the other hand, is neutralized, leaving full facial control to the face signal.

Face signal. Instead of using parameters from a 3DMM, we adopt the pretrained expression encoder from DPE [44] to extract pose-agnostic expressions from portrait images. Unlike 3DMMs [36, 47] trained from untextured scan meshes, the latent space that 2D talking faces methods like DPE [44] constructed from a large number of images is more expressive to capture the expression-related appearance variations.

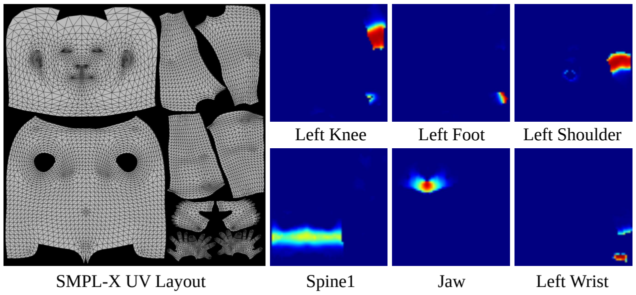

Figure 3. **Tiling and masking of Pose $\boldsymbol{\theta}$ Embedding.** Joint angles are filled to corresponding areas in the UV layout where the joints can affect through skinning. Colors visualize the skinning weights, which are converted to binary masks.

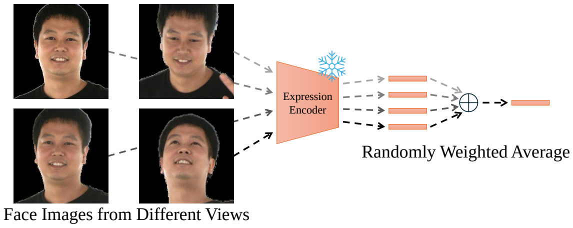

Figure 4. **Training with faces from multiviews.** During training, we extract expressions from multiple views and use a randomly averaged latent code as the face signal.

3.3. Conditional Variational Autoencoder

Given synchronized multiview images and registered SMPL-X of one frame, we neutralize the jaw pose and expression parameters and encode the body pose $\boldsymbol{\theta}$ with three encoders. Injected with a face signal from the expression encoder, the mixed driving signal is fed to a convolutional decoder for the generation of Gaussian parameters. Figure 2 illustrates the pipeline.

Pose $\boldsymbol{\theta}$ Embedding. The first encoder takes as input the pose vector $\boldsymbol{\theta} \in \mathbb{R}^{162}$ from SMPL-X with 54 joint angles, excluding the root joint for global orientation. We follow the practice of CABody [2] to expand the vector by 64×64 and then mask by downsized skinning maps from UV. This encoding scheme sets each pose component to the UV layout only where its corresponding joint affects. We visualize where the joints' $\boldsymbol{\theta}$ are filled to in Figure 3.

Posed Vertex Map Encoders. Another two encoders process the posed vertex map on UV. The first convolution encoder, referred to as the Posed Vertex Map (PVM) Encoder, encodes the posed vertex map down to resolution 64×64, matching that of the pose $\boldsymbol{\theta}$ encoding. The second, referred to as the Posed Vertices Embedding (PVE) Encoder, encodes the posed vertex map as a latent code, which we believe better captures the global information of the pose. The encoded features from the above three branches are concatenated as the final pose feature.

Expression Encoder. DPE [44] proposes a bidirectional cyclic training strategy in the training process aiming at the disentanglement of pose and expression. We take the pretrained expression encoder as our facial controller. From the input multiview images, we apply the head pose estimator from SynergyNet [63] to find front-facing views. In the training stage, we choose the four most frontal views to extract expression codes. For every iteration, a randomly weighted average of the four codes is used as the face signal, as illustrated in Figure 4.

Face Signal Injection. The expression code is firstly reformed by a fully connected layer and a small convolutional decoder to the resolution of 32×32. Then it is used to replace the top-left quarter of the pose feature. In the UV layout of SMPL-X, the top-left quarter corresponds to the face region. After the injection, we feed the mixed feature to a convolutional decoder for extracting Gaussian maps with pose-dependent corrections for position $\Delta\boldsymbol{\mu}$, rotation $\Delta\boldsymbol{q}$, and scaling $\Delta\boldsymbol{s}$, as well as pose-independent opacity o, and color $\boldsymbol{c}$.

3.4. Gaussian Maps and LBS

We define the base Gaussian Maps in SMPL-X's UV layout. The SMPL-X mesh in T-Pose is rasterized to UV as the base positions $\overline{\boldsymbol{\mu}}$, i.e., every valid pixel on UV represents one 3D Gaussian primitive in the canonical space. Similar to D3GA [79], we find every Gaussian primitive's corresponding triangle on the mesh to initialize its base rotation $\overline{\boldsymbol{q}}$, such that each Gaussian will have its first row axes aligned with the mesh surface and the third with the normal. The base scaling $\overline{\boldsymbol{s}}$ is initialized by treating the base positions as a regular point cloud.

Given the barycentric-interpolated skinning weights $\mathcal{W}$ from SMPL-X mesh, we apply the pose-dependent corrections in the canonical space, and calculate the Gaussian primitives' posed position $\boldsymbol{\mu}_p$ and rotation $\boldsymbol{q}_p$ by LBS:

$$\boldsymbol{\mu}_p = LBS_{Rt}(\overline{\boldsymbol{\mu}} + \Delta\boldsymbol{\mu}, \boldsymbol{\theta}, \mathcal{W}) \tag{6}$$

$$\boldsymbol{q}_p = LBS_{R}(\overline{\boldsymbol{q}} + \Delta\boldsymbol{q}, \boldsymbol{\theta}, \mathcal{W}) \tag{7}$$

$$\boldsymbol{s} = \overline{\boldsymbol{s}} + \Delta\boldsymbol{s} \tag{8}$$

As in the 3DGS rendering pipeline, the Gaussian primitives in the posed space $G = (\boldsymbol{\mu}_p, \boldsymbol{q}_p, \boldsymbol{s}, o, \boldsymbol{c})$ are splatted onto a 2D image as the final rendering.

3.5. Loss and Training

In the training process, DEGAS is supervised with photometric loss of $\mathcal{L}_1$, $\mathcal{L}_{ssim}$, and $\mathcal{L}_{lpips}$ [73]. The pose-dependent position $\Delta\boldsymbol{\mu}$ is regularized by an offset loss. To help convergency, we also introduce a regularization $\mathcal{L}_s$ on scaling to prevent any Gaussians from becoming too large (10x larger than its base scaling):

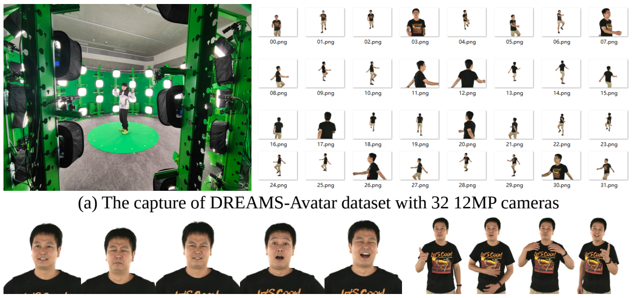
(a) The capture of DREAMS-Avatar dataset with 32 12MP cameras

(b) Captured expressions rendered by DEGAS

(c) Rendered talking footage

Figure 5. **The DREAMS-Avatar dataset.** 6 subjects captured with 32 12MP cameras performing large body poses and rich facial expressions, e.g., smiling, laughing, angry, surprised, and a sequence of talking or singing.

$$\begin{aligned}\mathcal{L} = (1-\lambda_{ssim})\mathcal{L}_1 + \lambda_{ssim}\mathcal{L}_{ssim} + \lambda_{lpips}\mathcal{L}_{lpips} \\ + \lambda_{\boldsymbol{\mu}}\left\|\Delta\boldsymbol{\mu}\right\|_2 + \lambda_s\mathcal{L}_s\end{aligned} \tag{9}$$

$$\mathcal{L}_s(i) = \begin{cases} |\boldsymbol{s}_i|, & \boldsymbol{s}_i > 10\overline{\boldsymbol{s}}_i \\ 0, & otherwise \end{cases} \tag{10}$$

where $\lambda_{ssim} = 0.2$, $\lambda_{lpips} = 0.1$, $\lambda_{\boldsymbol{\mu}} = 0.001$, and $\lambda_s = 1.0$ all through the experiments. We train DEGAS with Adam [32] for 800k iterations.

4. Experiments

ActorsHQ Dataset. ActorsHQ is a high-quality dataset for full-body avatars. We follow the experiment setup of AnimatableGaussians [38] to use 47 full-body views (46 views for training and 1 for testing, at 1k resolution).

DREAMS-Avatar Dataset. Due to the lack of datasets for evaluating full-body talking avatars with rich facial expressions, we propose the *DREAMS-Avatar* dataset. DREAMS-Avatar includes the performance of 6 subjects captured with 32 12MP cameras, each with 2 sequences. The first of which is the footage of standard poses and facial expressions, while the second is a freestyle talking or singing. We show in Figures 1 and 5 the large body poses, rich facial expressions, and challenging clothes and glasses in the dataset. We aim to cover the pose and expression variations in a tele-presentation scenario.

4.1. Comparison on Full-body Avatars

We conducted experiments on ActorsHQ in comparison to state-of-the-art (SoTA) methods including 3DGS-Avatar [53], GaussianAvatar [25], and AnimatableGaussians [38]. Different from well-aligned 3DMMs available in a multi-view head avatar dataset [33], registration in a

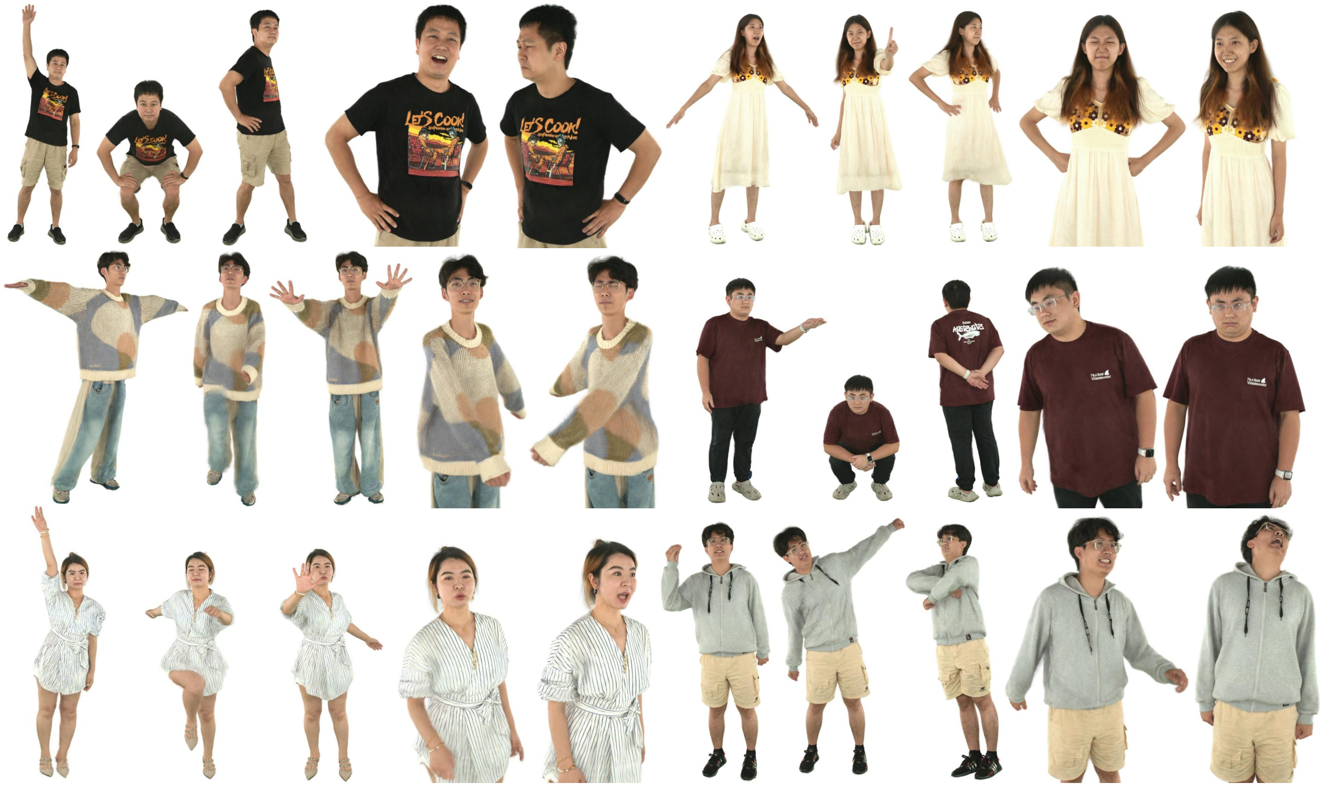

Figure 6. **Rendering results of our method.** We show rendering results of our method DEGAS on the DREAMS-Avatar dataset. DEGAS is able to render high quality avatars with large body pose variations and rich facial expression details.

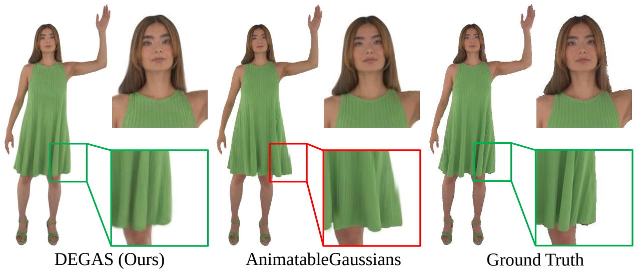

Figure 7. **Comparison on full-body avatars.** Our method renders high quality details on ActorsHQ.

Method	PSNR↑	SSIM↑	LPIPS↓	FID↓
GaussianAvatar [25]	26.9497	0.9389	0.0407	38.5387
3DGS-Avatar [53]	28.7836	0.9511	0.0418	49.3673
AnimatableGaussians [38]	<u>30.3607</u>	<u>0.9682</u>	<u>0.0339</u>	<u>33.4665</u>
Ours	**31.1262**	**0.9708**	**0.0318**	**24.4555**

Table 1. **Quantitative comparison on full-body avatars.** Experiments conducted on ActorsHQ Actor01/Sequence1 following the setup of AnimatableGaussians [38]. Our method quantitatively outperforms all three SoTA methods.

full-body setup is usually compromised by clothing (inaccurate surface alignment), large poses (inaccurate joints), moving head (inaccurate face alignment), etc.

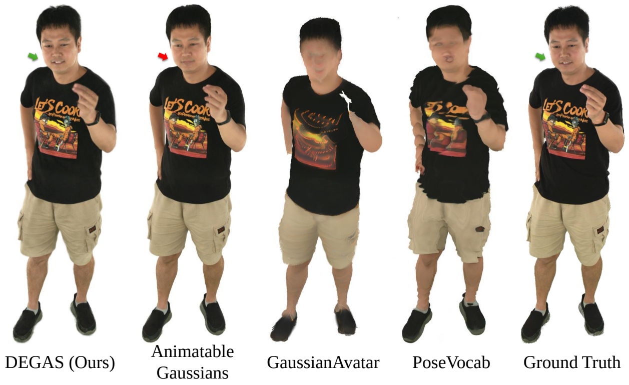

Figure 8. **Comparison on our DREAMS-Avatar dataset.** Our method renders high quality details comparing to SoTA methods.

Figure 7 shows the qualitative comparison on ActorsHQ. The rendering results of our method exhibit rich texture details. The quantitative comparison is reported in Table 1. We report PSNR and SSIM calculated in the rendered full images, LPIPS [73] and FID [23] in the cropped regions. Our method quantitatively outperforms all three SoTA methods. One key observation we make is that the adoption of powerful 2D CNN networks in both AnimatableGaussians [38] and ours significantly improves pose-dependent modeling. More discussions are in Section 4.3.

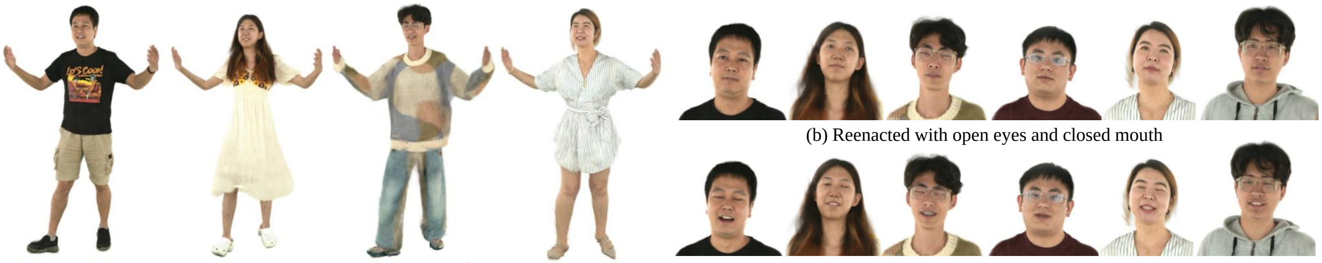

(a) All reenacted by Subject1 on the left

(b) Reenacted with open eyes and closed mouth

(c) Reenacted with closed eyes and open mouth

Figure 9. **Reenactment results of our method.** We show the rendering results of all subjects reenacted by Subject1's Sequence2. Most subjects are reenacted correctly on eyes and mouths except that Subject4's eyes control was affected by the reflections on the glasses.

Method	PSNR↑	SSIM↑	LPIPS↓	FID↓	AED↓
AnimatableGaussians [38]	32.1534	0.9814	0.0167	**13.0829**	0.2657
PoseVocab [37]	28.3966	0.9740	0.0503	147.1550	-
GaussianAvatar [25]	20.9320	0.9582	0.1056	81.0665	-
DEGAS (ours)	**33.9613**	**0.9853**	**0.01520**	13.9276	**0.0598**

Table 2. **Quantitative comparison on DREAMS-Avatar.** Our method outperforms other SoTA methods in terms of PSNR, SSIM, and LPIPS, and has on-par FID with AnimatableGaussians [38]. Expression accuracy AED of our method is significantly better. PoseVocab [37] and GaussianAvatar [25] failed to reconstruct the face region in the DREAMS-Avatar dataset.

4.2. Comparison on DREAMS-Avatar

For the experiments conducted on DREAMS-Avatar, we take Sequence1 of each subject for training with 31 cameras excluding Cam02, which is used only for testing. We evaluate view synthesis on Sequence1, novel pose and facial expression reenactment on Sequence2.

View Synthesis. Table 2 shows the quantitative results of view synthesis on Sequence1 Cam02's 500–1000 frames where both large poses and rich facial expressions are performed. The facial expression accuracy is evaluated by the *Average Expression Distance* (AED) proposed in PIRenderer [54], which estimates the cosine distance of the expression coefficients extracted by Deep3DFaceRecon [12]. We show the qualitative comparison in Figure 8. AnimatableGaussians [38] can render a high-quality body and a neutral face. PoseVocab [37] and GaussianAvatar [25] fail to model the face region due to the large expression variations in the dataset. While our method renders high-quality body and face details. We show more rendering results of DEGAS in Figure 6 with various poses and rich facial expressions.

Novel Poses and Expressions. We demonstrate the reenactment of DEGAS to novel poses. As shown in Figure 9, all avatars trained are reenacted by Subject1's Sequence2. Both same-identity and cross-identity reenactments show high-quality details. Specifically on the face regions, DEGAS responds correctly to eyes and mouth control.

Method	FPS↑	Training Time↓	Disentangled Encoder/Decoder
AnimatableGaussians [38]	10	160 hours	×
DEGAS (ours)	**30**	55 hours	✓

Table 3. **Comparison with AnimatableGaussians [38].** Our method reaches real-time framerate and favors disentangled encoder and decoder which contribute to potential applications. Numbers recorded on one NVIDIA RTX3090 and training with 800k iterations according to the original paper of AnimatableGaussians [38].

	Same-Identity Reenactment				Cross-Identity
	PSNR↑	SSIM↑	LPIPS↓	AED↓	AED↓
w/ DECA	26.185	0.954	0.049	0.1105	0.2638
w/ DAD-3DHeads	26.233	0.954	0.049	0.0998	0.3697
w/ DPE (ours)	26.212	0.954	0.049	**0.0853**	**0.2413**

Table 4. **Choice of face signal.** The 2D talking faces-based expression encoder from DPE [44] is a better choice as face signals.

4.3. Discussion w.r.t. AnimatableGaussians

Both our method and AnimatableGaussians [38] learn from CodecAvatars [2] in adopting powerful 2D CNN networks for the generation of Gaussian maps. The difference is that ours does not use skip connections between encoder and decoder, considering the potential streaming scenario [40]. Also, the bottleneck between the encoder and decoder that follows the UV layout of SMPL-X enables the face signal injection in our method. The runtime is compared in Table 3 where our method reaches a real-time framerate.

4.4. Ablation Study

Choice of face signal. We conducted ablation experiments to validate the design choice of using a pretrained expression encoder from DPE [44] as the face signal. We compared to using a 3DMM as the face signal by extracting FLAME parameters from the frontal camera. We replaced the *jaw pose* of SMPL-X with that from the extracted FLAME parameters and used the *expression* parameters to condition our convolutional decoder. Note that in our method, the *jaw pose* is neutralized, i.e., the jaw move-

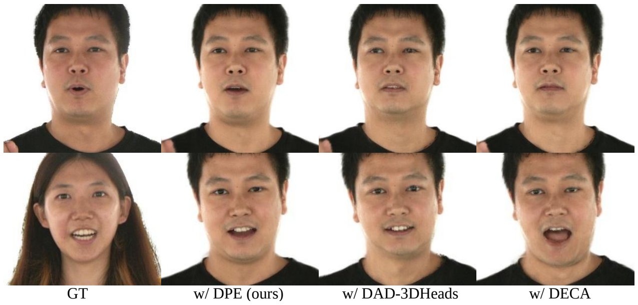

Figure 10. **Ablation on facial reenactment.** Using expression encoder from DPE [44] drives more similar expressions comparing to using DECA [17] or DAD-3DHeads [41].

	PSNR↑	SSIM↑	LPIPS↓	FID↓
3 views	29.6554	0.9748	0.0262	33.4759
6 views	30.9780	0.9782	0.0188	36.6235
12 views	30.9518	0.9783	0.0189	22.7458
31 views	32.6349	0.9823	0.0166	14.2061

Table 5. **Training with sparse views.** Our method can be trained with sparse views with decent quality.

	PSNR↑	SSIM↑	LPIPS↓	FID↓
w/o Pose $\boldsymbol{\theta}$ Embedding	30.0084	0.9695	0.0289	23.8262
w/o PVM Encoder	30.4173	0.9729	0.0284	24.2348
w/o PVE Encoder	29.4263	0.9656	0.0338	26.5531
Ours	**30.6700**	**0.9731**	**0.0281**	**23.8110**

Table 6. **Ablation on encoder branches.** All three encoder branches help improve the rendering quality of our method.

ments are solely represented by the cVAE.

We tested two approaches for extracting FLAME parameters, i.e., DECA [17] and DAD-3DHeads [41]. For same-identity reenactment, we trained on Subject1 Sequence1 and tested on Sequence2. For cross-identity reenactment, we reenacted the avatar by the motion of Subject2 Sequence2. As shown in Figure 10, the 2D talking faces-based expression encoder from DPE [44] enables more similar expressions. Table 4 shows the quantitative comparison.

Training with Sparse Views. Our avatar modeling method is trained in a multi-view setup. We report in Table 5 that DEGAS can be trained with 3 views, 6 views, and 12 views.

Pose Encoders. There are three pose encoders in our method to generate body signals. We conducted ablation studies on ActorsHQ Actor02 by disabling one of them each time. The quantitative results are reported in Table 6.

4.5. 3D Full-body Talking Avatars

The use of a pretrained encoder from 2D talking faces lets our method inherit the ability to both video-driven and audio-driven reenactment. With the help of SadTalker [74], we show the extension of DEGAS to full-body talking avatars. Given an audio clip, we firstly use SadTalker [74] to generate 2D talking videos from one face image of the subject, and then use the DPE [44] expression encoder to extract face signal to drive our avatars. The body pose generation is a whole another research track [9, 43, 69]. Here we only showcase the generation from TalkSHOW [69] in Figure 11. Noted that the *jaw pose* generated by TalkSHOW is not used.

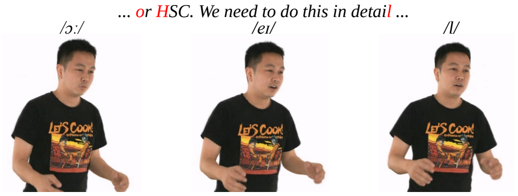

Figure 11. **Audio-driven example of our method.** Given an audio sequence, we generate face signal from SadTalker [74] and DPE [44], and body signal from TalkSHOW [69].

4.6. Limitations

The pretrained expression encoder from DPE [44] that we explore in this paper has the advantage of being trained with a large collection of face images. Yet the quality of the 2D talking faces method itself limits the reenactment quality of our method. We do observe pose and identity-related information being not fully disentangled from the expression. We believe that using encoders from more advanced 2D talking faces methods [68] would help. Another issue is that the clothes are not modeled in a separate layer, causing artifacts for the loose cloth in challenging poses.

5. Conclusion

In this paper, we proposed DEGAS, the first 3DGS-based method for full-body avatars with subtle and accurate facial expressions. We discussed in this paper that an expression latent space pretrained solely on 2D talking faces, is a better choice for the reenactment of 3D avatars, opening new possibilities for interactive life-like agents. The avatars modeled with DEGAS can be animated and rendered in real-time framerate to perform natural body motions and rich facial expressions. We conducted qualitative and quantitative experiments to validate the efficacy of our method. We also showed the audio-driven extension of our method to demonstrate its potential for downstream applications.

6. Acknowledgments

We thank the HKUST(GZ) DREAMS Lab for assisting in data collection. The work is supported by the National Social Science Foundation of China under grant number 24VWB020.

References

[1] Aneja, Shivangi and Thies, Justus and Dai, Angela and Nießner, Matthias. FaceTalk: Audio-Driven Motion Diffusion for Neural Parametric Head Models. In *Proceedings of the IEEE/CVF Conference on Computer Vision and Pattern Recognition (CVPR)*, pages 21263–21273, 2024. 2

[2] Timur Bagautdinov, Chenglei Wu, Tomas Simon, Fabián Prada, Takaaki Shiratori, Shih-En Wei, Weipeng Xu, Yaser Sheikh, and Jason Saragih. Driving-Signal Aware Full-Body Avatars. *ACM Trans. Graph.*, 40(4), 2021. 2, 3, 4, 7

[3] Elisabetta Bevacqua, Ken Prepin, Radoslaw Niewiadomski, Etienne de Sevin, and Catherine Pelachaud. Greta: Towards an Interactive Conversational Virtual Companion. *Artificial Companions in Society: Perspectives on the Present and Future*, pages 1–17, 2010. 1

[4] Changpeng Cai, Guinan Guo, Jiao Li, Junhao Su, Chenghao He, Jing Xiao, Yuanxu Chen, Lei Dai, and Feiyu Zhu. Listen, Disentangle, and Control: Controllable Speech-Driven Talking Head Generation. *arXiv preprint arXiv:2405.07257*, 2024. 3

[5] Xu Chen, Yufeng Zheng, Michael J. Black, Otmar Hilliges, and Andreas Geiger. SNARF: Differentiable Forward Skinning for Animating Non-Rigid Neural Implicit Shapes. In *Proceedings of the IEEE/CVF International Conference on Computer Vision (ICCV)*, pages 11594–11604, 2021. 3

[6] Xu Chen, Tianjian Jiang, Jie Song, Max Rietmann, Andreas Geiger, Michael J. Black, and Otmar Hilliges. Fast-SNARF: A Fast Deformer for Articulated Neural Fields. *Pattern Analysis and Machine Intelligence (PAMI)*, 2023. 3

[7] Yue Chen, Xuan Wang, Xingyu Chen, Qi Zhang, Xiaoyu Li, Yu Guo, Jue Wang, and Fei Wang. UV Volumes for Real-time Rendering of Editable Free-view Human Performance. In *Proceedings of the IEEE/CVF Conference on Computer Vision and Pattern Recognition (CVPR)*, pages 16621–16631, 2023. 3

[8] Kun-Hung Cheng and Chin-Chung Tsai. Children and Parents' Reading of An Augmented Reality Picture Book: Analyses of Behavioral Patterns and Cognitive Attainment. *Computers & Education*, 72:302–312, 2014. 1

[9] Kiran Chhatre, Radek Daněček, Nikos Athanasiou, Giorgio Becherini, Christopher Peters, Michael J. Black, and Timo Bolkart. AMUSE: Emotional Speech-Driven 3D Body Animation via Disentangled Latent Diffusion. In *Proceedings of the IEEE/CVF Conference on Computer Vision and Pattern Recognition (CVPR)*, pages 1942–1953, 2024. 8

[10] Collet, Alvaro and Chuang, Ming and Sweeney, Pat and Gillett, Don and Evseev, Dennis and Calabrese, David and Hoppe, Hugues and Kirk, Adam and Sullivan, Steve. High-Quality Streamable Free-Viewpoint Video. *ACM Trans. Graph.*, 34(4), 2015. 3

[11] Daniel Cudeiro, Timo Bolkart, Cassidy Laidlaw, Anurag Ranjan, and Michael Black. Capture, Learning, and Synthesis of 3D Speaking Styles. In *Proceedings IEEE Conf. on Computer Vision and Pattern Recognition (CVPR)*, pages 10101–10111, 2019. 3

[12] Yu Deng, Jiaolong Yang, Sicheng Xu, Dong Chen, Yunde Jia, and Xin Tong. Accurate 3D Face Reconstruction with Weakly-Supervised Learning: From Single Image to Image Set. In *IEEE Computer Vision and Pattern Recognition Workshops*, 2019. 7

[13] Junting Dong, Qi Fang, Yudong Guo, Sida Peng, Qing Shuai, Xiaowei Zhou, and Hujun Bao. TotalSelfScan: Learning Full-body Avatars from Self-Portrait Videos of Faces, Hands, and Bodies. In *Advances in Neural Information Processing Systems*, 2022. 3

[14] Michail Christos Doukas, Stefanos Zafeiriou, and Viktoriia Sharmanska. HeadGAN: One-Shot Neural Head Synthesis and Editing. In *Proceedings of the IEEE/CVF International Conference on Computer Vision (ICCV)*, pages 14398–14407, 2021. 3

[15] Nikita Drobyshev, Jenya Chelishev, Taras Khakhulin, Aleksei Ivakhnenko, Victor Lempitsky, and Egor Zakharov. Megaportraits: One-shot Megapixel Neural Head Avatars. In *Proceedings of the 30th ACM International Conference on Multimedia*, pages 2663–2671, 2022. 2

[16] Yingruo Fan, Zhaojiang Lin, Jun Saito, Wenping Wang, and Taku Komura. FaceFormer: Speech-Driven 3D Facial Animation with Transformers. In *Proceedings of the IEEE/CVF Conference on Computer Vision and Pattern Recognition (CVPR)*, 2022. 2, 3

[17] Yao Feng, Haiwen Feng, Michael J. Black, and Timo Bolkart. Learning an Animatable Detailed 3D Face Model from In-The-Wild Images. In *ACM Transactions on Graphics, (Proc. SIGGRAPH)*, 2021. 2, 8

[18] Ian Goodfellow, Jean Pouget-Abadie, Mehdi Mirza, Bing Xu, David Warde-Farley, Sherjil Ozair, Aaron Courville, and Yoshua Bengio. Generative Adversarial Nets. *Advances in Neural Information Processing Systems*, 27, 2014. 3

[19] Yudong Guo, Keyu Chen, Sen Liang, Yong-Jin Liu, Hujun Bao, and Juyong Zhang. Ad-NeRF: Audio Driven Neural Radiance Fields for Talking Head Synthesis. In *Proceedings of the IEEE/CVF International Conference on Computer Vision (ICCV)*, pages 5784–5794, 2021. 3

[20] Marc Habermann, Lingjie Liu, Weipeng Xu, Michael Zollhoefer, Gerard Pons-Moll, and Christian Theobalt. Real-time Deep Dynamic Characters. *ACM Transactions on Graphics (ToG)*, 40(4):1–16, 2021. 3

[21] Marc Habermann, Lingjie Liu, Weipeng Xu, Gerard Pons-Moll, Michael Zollhoefer, and Christian Theobalt. HDHumans: A Hybrid Approach for High-Fidelity Digital Humans. *Proc. ACM Comput. Graph. Interact. Tech.*, 6(3), 2023. 3

[22] Jennifer Healey, Duotun Wang, Curtis Wigington, Tong Sun, and Huaishu Peng. A Mixed-Reality System to Promote Child Engagement in Remote Intergenerational Storytelling. In *2021 IEEE International Symposium on Mixed and Augmented Reality Adjunct (ISMAR-Adjunct)*, pages 274–279, 2021. 1

[23] Martin Heusel, Hubert Ramsauer, Thomas Unterthiner, Bernhard Nessler, and Sepp Hochreiter. GANs Trained By a Two Time-Scale Update Rule Converge to a Local Nash Equilibrium. In *Proceedings of the 31st International Conference on Neural Information Processing Systems*, page 6629–6640, Red Hook, NY, USA, 2017. Curran Associates Inc. 6

[24] Hsuan-I Ho, Lixin Xue, Jie Song, and Otmar Hilliges. Learning Locally Editable Virtual Humans. In *Proceedings of the IEEE/CVF Conference on Computer Vision and Pattern Recognition (CVPR)*, pages 21024–21035, 2023. 3

[25] Liangxiao Hu, Hongwen Zhang, Yuxiang Zhang, Boyao Zhou, Boning Liu, Shengping Zhang, and Liqiang Nie. GaussianAvatar: Towards Realistic Human Avatar Modeling from a Single Video via Animatable 3D Gaussians. In *Proceedings of the IEEE/CVF Conference on Computer Vision and Pattern Recognition (CVPR)*, 2024. 1, 3, 5, 6, 7

[26] Shoukang Hu, Tao Hu, and Ziwei Liu. Gauhuman: Articulated Gaussian Splatting from Monocular Human Videos. In *Proceedings of the IEEE/CVF Conference on Computer Vision and Pattern Recognition (CVPR)*, pages 20418–20431, 2024. 3

[27] Tao Hu, Fangzhou Hong, and Ziwei Liu. SurMo: Surface-Based 4D Motion Modeling for Dynamic Human Rendering. In *Proceedings of the IEEE/CVF Conference on Computer Vision and Pattern Recognition (CVPR)*, pages 6550–6560, 2024. 3

[28] Phillip Isola, Jun-Yan Zhu, Tinghui Zhou, and Alexei A Efros. Image-to-Image Translation with Conditional Adversarial Networks. In *Proceedings of the IEEE Conference on Computer Vision and Pattern Recognition (CVPR)*, pages 1125–1134, 2017. 3

[29] Jiang, Tianjian and Chen, Xu and Song, Jie and Hilliges, Otmar. InstantAvatar: Learning Avatars From Monocular Video in 60 Seconds. In *Proceedings of the IEEE/CVF Conference on Computer Vision and Pattern Recognition (CVPR)*, pages 16922–16932, 2023. 1, 3

[30] Redouane Kachach, Pablo Perez, Alvaro Villegas, and Ester Gonzalez-Sosa. Virtual Tour: An Immersive Low Cost Telepresence System. In *2020 IEEE Conference on Virtual Reality and 3D User Interfaces Abstracts and Workshops (VRW)*, pages 504–506, 2020. 1

[31] Bernhard Kerbl, Georgios Kopanas, Thomas Leimkühler, and George Drettakis. 3D Gaussian Splatting for Real-Time Radiance Field Rendering. *ACM Transactions on Graphics*, 42(4), 2023. 1, 2, 4

[32] Diederik Kingma and Jimmy Ba. Adam: A Method for Stochastic Optimization. In *International Conference on Learning Representations (ICLR)*, San Diega, CA, USA, 2015. 5

[33] Tobias Kirschstein, Shenhan Qian, Simon Giebenhain, Tim Walter, and Matthias Nießner. NeRSemble: Multi-View Radiance Field Reconstruction of Human Heads. *ACM Trans. Graph.*, 42(4), 2023. 5

[34] Nianlong Li, Zhengquan Zhang, Can Liu, Zengyao Yang, Yinan Fu, Feng Tian, Teng Han, and Mingming Fan. VMirror: Enhancing the Interaction with Occluded or Distant Objects in VR with Virtual Mirrors. In *Proceedings of the 2021 CHI Conference on Human Factors in Computing Systems*, New York, NY, USA, 2021. Association for Computing Machinery. 1

[35] Ruilong Li, Julian Tanke, Minh Vo, Michael Zollhofer, Jurgen Gall, Angjoo Kanazawa, and Christoph Lassner. TAVA: Template-Free Animatable Volumetric Actors. In *European Conference on Computer Vision (ECCV)*, 2022. 3

[36] Tianye Li, Timo Bolkart, Michael. J. Black, Hao Li, and Javier Romero. Learning a Model of Facial Shape and Expression from 4D Scans. *ACM Transactions on Graphics, (Proc. SIGGRAPH Asia)*, 36(6):194:1–194:17, 2017. 2, 3, 4

[37] Zhe Li, Zerong Zheng, Yuxiao Liu, Boyao Zhou, and Yebin Liu. PoseVocab: Learning Joint-Structured Pose Embeddings for Human Avatar Modeling. In *ACM SIGGRAPH Conference Proceedings*, 2023. 3, 7

[38] Zhe Li, Zerong Zheng, Lizhen Wang, and Yebin Liu. Animatable Gaussians: Learning Pose-Dependent Gaussian Maps for High-Fidelity Human Avatar Modeling. In *Proceedings of the IEEE/CVF Conference on Computer Vision and Pattern Recognition (CVPR)*, 2024. 1, 2, 3, 5, 6, 7

[39] Loper, Matthew and Mahmood, Naureen and Romero, Javier and Pons-Moll, Gerard and Black, Michael J. SMPL: A Skinned Multi-Person Linear Model. *ACM Trans. Graph.*, 34(6), 2015. 3

[40] Shugao Ma, Tomas Simon, Jason Saragih, Dawei Wang, Yuecheng Li, Fernando De la Torre, and Yaser Sheikh. Pixel Codec Avatars. In *Proceedings of the IEEE/CVF Conference on Computer Vision and Pattern Recognition (CVPR)*, pages 64–73, 2021. 3, 7

[41] Tetiana Martyniuk, Orest Kupyn, Yana Kurlyak, Igor Krashenyi, Jiři Matas, and Viktoriia Sharmanska. DAD-3DHeads: A Large-scale Dense, Accurate and Diverse Dataset for 3D Head Alignment from a Single Image. In *Proc. IEEE Conf. on Computer Vision and Pattern Recognition (CVPR)*, 2022. 2, 8

[42] Ben Mildenhall, Pratul P. Srinivasan, Matthew Tancik, Jonathan T. Barron, Ravi Ramamoorthi, and Ren Ng. NeRF: Representing Scenes as Neural Radiance Fields for View Synthesis. In *Computer Vision – ECCV 2020: 16th European Conference, Glasgow, UK, August 23–28, 2020, Proceedings, Part I*, page 405–421, Berlin, Heidelberg, 2020. Springer-Verlag. 1

[43] Evonne Ng, Javier Romero, Timur Bagautdinov, Shaojie Bai, Trevor Darrell, Angjoo Kanazawa, and Alexander Richard. From Audio to Photoreal Embodiment: Synthesizing Humans in Conversations. In *IEEE Conference on Computer Vision and Pattern Recognition (CVPR)*, 2024. 2, 3, 8

[44] Youxin Pang, Yong Zhang, Weize Quan, Yanbo Fan, Xiaodong Cun, Ying Shan, and Dong-Ming Yan. DPE: Disentanglement of Pose and Expression for General Video Portrait Editing. In *Proceedings of the IEEE/CVF Conference on Computer Vision and Pattern Recognition (CVPR)*, pages 427–436, 2023. 2, 3, 4, 5, 7, 8

[45] Pang, Haokai and Zhu, Heming and Kortylewski, Adam and Theobalt, Christian and Habermann, Marc. Ash: Animatable gaussian splats for efficient and photoreal human rendering. In *Proceedings of the IEEE/CVF Conference on Computer Vision and Pattern Recognition (CVPR)*, pages 1165–1175, 2024. 3

[46] Georgios Pavlakos, Vasileios Choutas, Nima Ghorbani, Timo Bolkart, Ahmed A. A. Osman, Dimitrios Tzionas, and Michael J. Black. Expressive Body Capture: 3D Hands, Face, and Body from a Single Image. In *Proceedings of the IEEE/CVF Conference on Computer Vision and Pattern Recognition (CVPR)*, 2019. 2, 3

[47] Pascal Paysan, Reinhard Knothe, Brian Amberg, Sami Romdhani, and Thomas Vetter. A 3D Face Model for Pose and Illumination Invariant Face Recognition. In *2009 sixth IEEE International Conference on Advanced Video and Signal Based Surveillance*, pages 296–301. Ieee, 2009. 2, 4

[48] Sida Peng, Yuanqing Zhang, Yinghao Xu, Qianqian Wang, Qing Shuai, Hujun Bao, and Xiaowei Zhou. Neural Body: Implicit Neural Representations with Structured Latent Codes for Novel View Synthesis of Dynamic Humans. In *Proceedings of the IEEE/CVF Conference on Computer Vision and Pattern Recognition (CVPR)*, 2021. 3

[49] Sida Peng, Chen Geng, Yuanqing Zhang, Yinghao Xu, Qianqian Wang, Qing Shuai, Xiaowei Zhou, and Hujun Bao. Implicit Neural Representations with Structured Latent Codes for Human Body Modeling. *IEEE Transactions on Pattern Analysis and Machine Intelligence*, 2023. 3

[50] Ziqiao Peng, Wentao Hu, Yue Shi, Xiangyu Zhu, Xiaomei Zhang, Jun He, Hongyan Liu, and Zhaoxin Fan. SyncTalk: The Devil is in The Synchronization for Talking Head Synthesis. In *Proceedings of the IEEE/CVF Conference on Computer Vision and Pattern Recognition (CVPR)*, 2024. 2, 3

[51] Ben Poole, Ajay Jain, Jonathan T. Barron, and Ben Mildenhall. DreamFusion: Text-to-3D using 2D Diffusion. *arXiv preprint arXiv:2209.14988*, 2022. 2

[52] Shenhan Qian, Tobias Kirschstein, Liam Schoneveld, Davide Davoli, Simon Giebenhain, and Matthias Nießner. GaussianAvatars: Photorealistic Head Avatars with Rigged 3D Gaussians. In *Proceedings of the IEEE/CVF Conference on Computer Vision and Pattern Recognition (CVPR)*, 2024. 1, 2, 3

[53] Zhiyin Qian, Shaofei Wang, Marko Mihajlovic, Andreas Geiger, and Siyu Tang. 3DGS-Avatar: Animatable Avatars via Deformable 3D Gaussian Splatting. In *Proceedings of the IEEE/CVF Conference on Computer Vision and Pattern Recognition (CVPR)*, 2024. 3, 5, 6

[54] Yurui Ren, Ge Li, Yuanqi Chen, Thomas H Li, and Shan Liu. Pirenderer: Controllable Portrait Image Generation via Semantic Neural Rendering. In *Proceedings of the IEEE/CVF international conference on computer vision*, pages 13759–13768, 2021. 3, 7

[55] Shunsuke Saito, Gabriel Schwartz, Tomas Simon, Junxuan Li, and Giljoo Nam. Relightable Gaussian Codec Avatars. In *Proceedings of the IEEE/CVF Conference on Computer Vision and Pattern Recognition (CVPR)*, 2024. 1, 3

[56] Zhijing Shao, Zhaolong Wang, Zhuang Li, Duotun Wang, Xiangru Lin, Yu Zhang, Mingming Fan, and Zeyu Wang. SplattingAvatar: Realistic Real-Time Human Avatars with Mesh-Embedded Gaussian Splatting. In *Proceedings of the IEEE/CVF Conference on Computer Vision and Pattern Recognition (CVPR)*, 2024. 1, 2, 3

[57] Kaiyue Shen, Chen Guo, Manuel Kaufmann, Juan Jose Zarate, Julien Valentin, Jie Song, and Otmar Hilliges. X-Avatar: Expressive Human Avatars. In *Proceedings of the IEEE/CVF Conference on Computer Vision and Pattern Recognition (CVPR)*, pages 16911–16921, 2023. 3

[58] Thambiraja, Balamurugan and Habibie, Ikhsanul and Aliakbarian, Sadegh and Cosker, Darren and Theobalt, Christian and Thies, Justus. Imitator: Personalized Speech-Driven 3D Facial Animation. In *Proceedings of the IEEE/CVF International Conference on Computer Vision (ICCV)*, pages 20621–20631, 2023. 2, 3

[59] Duotun Wang, Hengyu Meng, Zeyu Cai, Zhijing Shao, Qianxi Liu, Lin Wang, Mingming Fan, Ying Shan, Xiaohang Zhan, and Zeyu Wang. HeadEvolver: Text to Head Avatars via Locally Learnable Mesh Deformation. *arXiv preprint arXiv:2403.09326*, 2024. 2

[60] Shaofei Wang, Katja Schwarz, Andreas Geiger, and Siyu Tang. ARAH: Animatable Volume Rendering of Articulated Human SDFs. In *European Conference on Computer Vision (ECCV)*, 2022. 3

[61] Ting-Chun Wang, Ming-Yu Liu, Andrew Tao, Guilin Liu, Bryan Catanzaro, and Jan Kautz. Few-Shot Video-to-Video Synthesis. In *Advances in Neural Information Processing Systems*. Curran Associates, Inc., 2019. 3

[62] Ting-Chun Wang, Arun Mallya, and Ming-Yu Liu. One-Shot Free-View Neural Talking-Head Synthesis for Video Conferencing. In *Proceedings of the IEEE Conference on Computer Vision and Pattern Recognition (CVPR)*, 2021. 2

[63] Cho-Ying Wu, Qiangeng Xu, and Ulrich Neumann. Synergy between 3DMM and 3D Landmarks for Accurate 3D Facial Geometry. In *2021 International Conference on 3D Vision (3DV)*, pages 453–463, 2021. 5

[64] Wu, Guanjun and Yi, Taoran and Fang, Jiemin and Xie, Lingxi and Zhang, Xiaopeng and Wei, Wei and Liu, Wenyu and Tian, Qi and Wang, Xinggang. 4D Gaussian Splatting for Real-Time Dynamic Scene Rendering. In *Proceedings of the IEEE/CVF Conference on Computer Vision and Pattern Recognition (CVPR)*, pages 20310–20320, 2024. 3

[65] Jinbo Xing, Menghan Xia, Yuechen Zhang, Xiaodong Cun, Jue Wang, and Tien-Tsin Wong. Codetalker: Speech-Driven 3D Facial Animation with Discrete Motion Prior. In *Proceedings of the IEEE/CVF Conference on Computer Vision and Pattern Recognition (CVPR)*, pages 12780–12790, 2023. 2, 3

[66] Chao Xu, Yang Liu, Jiazheng Xing, Weida Wang, Mingze Sun, Jun Dan, Tianxin Huang, Siyuan Li, Zhi-Qi Cheng, Ying Tai, et al. FaceChain-ImagineID: Freely Crafting High-Fidelity Diverse Talking Faces from Disentangled Audio. In *Proceedings of the IEEE/CVF Conference on Computer Vision and Pattern Recognition (CVPR)*, pages 1292–1302, 2024. 3

[67] Mingwang Xu, Hui Li, Qingkun Su, Hanlin Shang, Liwei Zhang, Ce Liu, Jingdong Wang, Luc Van Gool, Yao Yao, and Siyu Zhu. Hallo: Hierarchical Audio-Driven Visual Synthesis for Portrait Image Animation. *arXiv preprint arXiv:2406.08801*, 2024. 3

[68] Sicheng Xu, Guojun Chen, Yu-Xiao Guo, Jiaolong Yang, Chong Li, Zhenyu Zang, Yizhong Zhang, Xin Tong, and Baining Guo. Vasa-1: Lifelike Audio-Driven Talking Faces Generated in Real Time. *arXiv preprint arXiv:2404.10667*, 2024. 2, 3, 8

[69] Hongwei Yi, Hualin Liang, Yifei Liu, Qiong Cao, Yandong Wen, Timo Bolkart, Dacheng Tao, and Michael J Black. Generating Holistic 3D Human Motion from Speech. In *Proceedings of the IEEE/CVF Conference on Computer Vision and Pattern Recognition (CVPR)*, 2023. 8

[70] Fei Yin, Yong Zhang, Xiaodong Cun, Mingdeng Cao, Yanbo Fan, Xuan Wang, Qingyan Bai, Baoyuan Wu, Jue Wang, and Yujiu Yang. Styleheat: One-Shot High-Resolution Editable Talking Face Generation via Pre-Trained Stylegan. In *European Conference on Computer Vision (ECCV)*, pages 85–101. Springer, 2022. 3

[71] Hongyun Yu, Zhan Qu, Qihang Yu, Jianchuan Chen, Zhonghua Jiang, Zhiwen Chen, Shengyu Zhang, Jimin Xu, Fei Wu, Chengfei Lv, et al. GaussianTalker: Speaker-Specific Talking Head Synthesis via 3D Gaussian Splatting. *arXiv preprint arXiv:2404.14037*, 2024. 3

[72] Runyi Yu, Tianyu He, Ailing Zeng, Yuchi Wang, Junliang Guo, Xu Tan, Chang Liu, Jie Chen, and Jiang Bian. Make Your Actor Talk: Generalizable and High-Fidelity Lip Sync with Motion and Appearance Disentanglement. *arXiv preprint arXiv:2406.08096*, 2024. 3

[73] Richard Zhang, Phillip Isola, Alexei A Efros, Eli Shechtman, and Oliver Wang. The Unreasonable Effectiveness of Deep Features as a Perceptual Metric. In *Proceedings of the IEEE Conference on Computer Vision and Pattern Recognition (CVPR)*, 2018. 5, 6

[74] Wenxuan Zhang, Xiaodong Cun, Xuan Wang, Yong Zhang, Xi Shen, Yu Guo, Ying Shan, and Fei Wang. Sadtalker: Learning Realistic 3D Motion Coefficients for Stylized Audio-Driven Single Image Talking Face Animation. In *Proceedings of the IEEE/CVF Conference on Computer Vision and Pattern Recognition (CVPR)*, pages 8652–8661, 2023. 2, 3, 8

[75] Yufeng Zheng, Wang Yifan, Gordon Wetzstein, Michael J Black, and Otmar Hilliges. Pointavatar: Deformable Point-Based Head Avatars from Videos. In *Proceedings of the IEEE/CVF Conference on Computer Vision and Pattern Recognition (CVPR)*, pages 21057–21067, 2023. 3

[76] Zerong Zheng, Han Huang, Tao Yu, Hongwen Zhang, Yandong Guo, and Yebin Liu. Structured Local Radiance Fields for Human Avatar Modeling. In *Proceedings of the IEEE/CVF Conference on Computer Vision and Pattern Recognition (CVPR)*, 2022. 3

[77] Zerong Zheng, Xiaochen Zhao, Hongwen Zhang, Boning Liu, and Yebin Liu. AvatarRex: Real-Time Expressive Full-Body Avatars. *ACM Transactions on Graphics (TOG)*, 42 (4), 2023. 3

[78] Wojciech Zielonka, Timo Bolkart, and Justus Thies. Towards Metrical Reconstruction of Human Faces. In *European Conference on Computer Vision (ECCV)*, 2022. 2

[79] Wojciech Zielonka, Timur Bagautdinov, Shunsuke Saito, Michael Zollhöfer, Justus Thies, and Javier Romero. Drivable 3D Gaussian Avatars. *arXiv preprint arXiv:2311.08581*, 2023. 2, 5

[80] Zielonka, Wojciech and Bolkart, Timo and Thies, Justus. Instant Volumetric Head Avatars. In *Proceedings of the IEEE/CVF Conference on Computer Vision and Pattern Recognition (CVPR)*, pages 4574–4584, 2023. 1, 3

[81] Matthias Zwicker, Hanspeter Pfister, Jeroen van Baar, and Markus Gross. Surface Splatting. In *Proceedings of the 28th Annual Conference on Computer Graphics and Interactive Techniques*, page 371–378, New York, NY, USA, 2001. Association for Computing Machinery. 4